ARTICLE IN PRESS

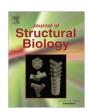
Journal of Structural Biology xxx (2015) xxx-xxx



Contents lists available at ScienceDirect

Journal of Structural Biology

journal homepage: www.elsevier.com/locate/yjsbi



X-ray recordings reveal how a human disease-linked skeletal muscle α -actin mutation leads to contractile dysfunction

Julien Ochala ^{a,*}, Gianina Ravenscroft ^b, Elyshia McNamara ^b, Kristen J. Nowak ^b, Hiroyuki Iwamoto ^c

- ^a Centre of Human and Aerospace Physiological Sciences, School of Biomedical Sciences, King's College London, London, United Kingdom
- ^b Harry Perkins Institute of Medical Research, The University of Western Australia, Nedlands, Australia

ARTICLE INFO

Article history: Received 16 May 2015 Received in revised form 13 August 2015 Accepted 22 September 2015 Available online xxxx

Keywords: Muscle disease Actin Myosin Small-angle X-ray scattering

ABSTRACT

In humans, mutant skeletal muscle α -actin proteins are associated with contractile dysfunction, skeletal muscle weakness and a wide range of primarily skeletal muscle diseases. Despite this knowledge, the exact molecular mechanisms triggering the contractile dysfunction remain unknown. Here, we aimed to unravel these. Hence, we used a transgenic mouse model expressing a well-described D286G mutant skeletal muscle α -actin protein and recapitulating the human condition of contractile deregulation and severe skeletal muscle weakness. We then recorded and analyzed the small-angle X-ray diffraction patterns of isolated membrane-permeabilized myofibers. Results showed that upon addition of Ca^{2^+} , the intensity changes of the second $(1/19~\text{nm}^{-1})$ and sixth $(1/5.9~\text{nm}^{-1})$ actin layer lines and of the first myosin meridional reflection $(1/14.3~\text{nm}^{-1})$ were disrupted when the thin-thick filament overlap was optimal (sarcomere length of $2.5-2.6~\text{\mu m}$). However these reflections were normal when the thin and thick filaments were not interacting (sarcomere length > $3.6~\text{\mu m}$). These findings demonstrate, for the first time, that the replacement of just one amino acid in the skeletal muscle α -actin protein partly prevents actin conformational changes during activation, disrupting the strong binding of myosin molecules. This leads to a limited myosin-related tropomyosin movement over the thin filaments, further affecting the amount of cross-bridges, explaining the contractile dysfunction.

© 2015 Elsevier Inc. All rights reserved.

1. Introduction

In humans, more than 200 different mutations in the gene encoding skeletal muscle α -actin (*ACTA1*) have been identified and are associated with a wide range of skeletal muscle diseases including nemaline myopathy, cap disease, core myopathy, congenital fiber type disproportion and intranuclear rod myopathy (Nowak et al., 2013, 1999). Despite this diversity, almost all share one common feature, namely detrimental muscle weakness affecting limb and respiratory muscles (Nowak et al., 2013, 1999). No cure exists for patients and treatment focuses on symptomatic management such as respiratory intervention, particularly nocturnal ventilation (Nowak et al., 2013, 1999). Possible therapeutic approaches could be guided by the exact molecular mechanisms

E-mail address: julien.ochala@kcl.ac.uk (J. Ochala).

http://dx.doi.org/10.1016/j.jsb.2015.09.008 1047-8477/© 2015 Elsevier Inc. All rights reserved. by which these ACTA1 mutations lead to muscle diseases, however this information is currently lacking.

Most ACTA1 mutations are relatively subtle, typically missense mutations modifying one DNA nucleotide. These in turn result in the substitution of just one residue in the skeletal muscle α -actin protein. Thus, understanding how such minor modifications induce muscle weakness, and more specifically contractile dysfunction, would give important insights into the pathophysiological phenomena. A few mouse models of ACTA1 disease have been developed (Nguyen et al., 2011; Ravenscroft et al., 2011), including one that carries a D286G mutation (Ravenscroft et al., 2011). Skeletal muscle weakness in these mice has been linked to contractile deregulation characterized by an inappropriate amount of strongly bound myosin cross-bridges and decreased forcegenerating capacity (Ochala et al., 2012).

In skeletal muscle, myosin binding to thin filaments depends on other contractile proteins, e.g., tropomyosin. Indeed, in the absence of Ca²⁺, tropomyosin sterically hinders interactions between actin and myosin molecules. Upon addition of Ca²⁺, tropomyosin moves over the surface of actin exposing myosin-binding sites on thin

^c Japan Synchrotron Radiation Research Institute, SPring8, Hyogo, Japan

^{*} Corresponding author at: Centre of Human & Aerospace Physiological Sciences, Faculty of Life Sciences and Medicine, King's College London, Room 3.3, Shepherd's House, Guy's Campus, London SE1 1UL, UK.

2

filaments, allowing the formation of strongly bound cross-bridges and the production of force (Lehman and Craig, 2008). One may hypothesize that D286G skeletal muscle α -actin alters some of the processes mentioned above. To investigate this, in the present study we recorded the X-ray diffraction patterns of single membrane-permeabilized myofibers from wild-type (WT) mice and from transgenic rodents expressing the D286G skeletal muscle α -actin mutation (referred to as D286G). We then monitored intensity changes during activation, and in various conditions. We measured the far off-meridional part of the second actin layer line (ALL) at $1/19~\text{nm}^{-1}$ (tropomyosin), sixth and seventh ALL at $1/5.9~\text{and}~1/5.1~\text{nm}^{-1}$, respectively (actin). We also measured the first myosin meridional reflection (MM), at $1/14.3~\text{nm}^{-1}$ (myosin) .

2. Materials and methods

2.1. Animals

The Animal Experimentation Ethics Committee of The University of Western Australia approved all animal procedures. Five 19-week old transgenic mice expressing skeletal muscle α -actin with the D286G variant (herein referred to as "D286G"; (Ravenscroft et al., 2013)) and five age- and gender-matched wild-type mice (referred to as "WT") were used in the present study. Mice were killed by cervical dislocation and tibialis anterior (TA) muscles were dissected.

2.2. Muscle preparation and myofiber permeabilization

TA muscles were placed in relaxing solution at 4 °C. Bundles of approximately 50 myofibers were dissected free and then tied with surgical silk to glass capillary tubes at slightly stretched lengths. They were then treated with skinning solution (relaxing solution containing glycerol; 50:50 v/v) for 24 h at 4 °C, after which they were transferred to -20 °C. In addition, the muscle bundles were treated with sucrose, a cryoprotectant, within 1–2 weeks for long-term storage (Frontera and Larsson, 1997). They were detached from the capillary tubes and snap frozen in liquid nitrogen-chilled propane and stored at -80 °C.

2.3. X-ray diffraction recordings and analyzes

Two to three days prior to X-ray recordings, bundles were de-sucrosed and transferred to a relaxing solution, and single myofibers were dissected. Arrays of approximately 30 fibers were prepared (Iwamoto, 2009; Iwamoto et al., 2001, 2002, 2003; Ochala et al., 2012, 2008, 2011). For each myofiber, both ends were clamped to half-split gold meshes for electron microscopy (width, 3 mm), which had been glued to precision-machined ceramic chips (width, 3 mm) designed to fit into a specimen chamber. The arrays were then transferred to the skinning solution and stored at −20 °C. On the day of the X-ray recordings, arrays were placed in a plastic dish containing a pre-activating solution and washed thoroughly to remove the glycerol. Arrays were then transferred to the specimen chamber, capable of manual length adjustment and force measurement (force transducer, AE801, Memscap, Bernin, France), filled with a pre-activating solution. Mean sarcomere length was measured and set to $2.5-2.6 \,\mu m$ or >3.6 μm . Subsequently, for arrays at a sarcomere length equal to 2.5–2.6 µm, X-ray diffraction patterns were recorded at 15 °C, first in the pre-activating solution and then in the activating solution (pCa 4.5) when maximal steady-state isometric force was reached. It should be mentioned that the activating solution was supplied to the chamber by using a remote-controlled pump. For arrays at a sarcomere length > 3.60 μm, the protocol was identical except that

pre-activating and activating solutions were replaced by low-EGTA rigor and calcium-rigor solutions with 2,3-butanedione monoxime (to prevent major sarcomere in-homogeneities). For each array, approximately 20-30 diffraction patterns were recorded (depending on fiber length) for each solution at the BL45XU beamline of SPring-8. The wavelength was 0.09 nm, and the specimen-todetector distance was 2 m. As a detector, a cooled CCD camera (C4880, Hamamatsu Photonics; 1000 × 1018 pixels) was used in combination with an image intensifier (VP5445, Hamamatsu Photonics). To minimize radiation damage, the exposure time was kept low (2 s), and the specimen chamber was moved 100 µm after each exposure. Moreover, we placed an aluminum plate (thickness, 0.35–0.5 mm) upstream of the specimen chamber. The beam flux was estimated to be between 2.7×10^{11} and 4.0×10^{11} photons/s after attenuation, and the beam size at the sample position was 0.2 mm (vertical) and 0.3 mm (horizontal). Following the X-ray recordings, background scattering was subtracted, and reflection intensities were determined as described elsewhere (Iwamoto, 2009; Iwamoto et al., 2001, 2002, 2003; Yagi, 2003).

2.4. Solutions

Relaxing and activating solutions contained 4 mM Mg-ATP, 1 mM free Mg²⁺, 20 mM imidazole, 7 mM EGTA, 14.5 mM creatine phosphate, 324 U/mL creatine phosphokinase, 1000 U/mL catalase, and KCl to adjust the ionic strength to 180 mM and pH to 7.0. Dithiothreitol (DTT) was also added. The pre-activating solution was identical to the relaxing solution, except that the EGTA concentration was reduced to 0.5 mM. The concentrations of free Ca²⁺ were $10^{-9.0}$ M (relaxing and pre-activating solutions) and $10^{-4.5}$ M (activating solutions). The rigor solution had similar compositions as the activating solution, except that MgATP, creatine phosphate, and creatine phosphokinase were absent.

3. Results and discussion

All the intensity changes during activation were successfully monitored and analyzed. The diffraction patterns are shown in Figs. 1 and 2. All intensities are summarized in Tables 1 and 2.

3.1. Preserved myofilament lattice

To prove that the myofilament lattice spacing was not affected by the presence of D286G skeletal muscle α -actin, we converted the 1,0 equatorial reflections to $d_{1,0}$ spacings using Bragg's Law (Colson et al., 2007). $d_{1,0}$ spacing and the widths of the 1,0 equatorial reflections ($\Delta_{1,0}$) did not appear different between WT and D286G myofibers (Table 1).

3.2. Aberrant actin structural changes

The sixth $(1/5.9~\text{nm}^{-1})$ and seventh $(1/5.1~\text{nm}^{-1})$ ALLs reflect the pitch of the left- and right-handed helices drawn through the actin monomers (Iwamoto, 2009). Upon addition of Ca^{2^+} , their intensities are usually greater. This is likely to arise from individual skeletal muscle α -actin molecules modifying their shape and their helical symmetry (Bordas et al., 1999; Wakabayashi et al., 1994) via an axial compression and a closing-up between subdomains 1 and 2 and between subdomains 3 and 4 (Iwamoto, 2009). In the present study, the intensification of the sixth ALL was less pronounced in D286G when compared with WT myofibers (–58%, Fig. 1 and Table 2). This suggests that the activation-induced structural change of skeletal muscle α -actin molecules is disrupted in the presence of the "poison" D286G. The mechanisms remain

Download English Version:

https://daneshyari.com/en/article/5913642

Download Persian Version:

https://daneshyari.com/article/5913642

<u>Daneshyari.com</u>